

Spatially anisotropic Heisenberg kagome antiferromagnet

This article has been downloaded from IOPscience. Please scroll down to see the full text article.

2007 J. Phys.: Condens. Matter 19 145255

(<http://iopscience.iop.org/0953-8984/19/14/145255>)

View [the table of contents for this issue](#), or go to the [journal homepage](#) for more

Download details:

IP Address: 129.252.86.83

The article was downloaded on 28/05/2010 at 17:33

Please note that [terms and conditions apply](#).

Spatially anisotropic Heisenberg kagome antiferromagnet

W Apel¹, T Yavors'kii² and H-U Everts³

¹ Physikalisch-Technische Bundesanstalt, Braunschweig, Germany

² Department of Physics, University of Waterloo, ON, Canada

³ Institut für Theoretische Physik, Universität Hannover, Hannover, Germany

E-mail: Walter.Apel@ptb.de

Received 17 August 2006

Published 23 March 2007

Online at stacks.iop.org/JPhysCM/19/145255

Abstract

In the search for spin-1/2 kagome antiferromagnets, the mineral volborthite has recently been the subject of experimental studies (Hiroi *et al* 2001 *J. Phys. Soc. Japan* **70** 3377; Fukaya *et al* 2003 *Phys. Rev. Lett.* **91** 207603; Bert *et al* 2004 *J. Phys.: Condens. Matter* **16** S829; Bert *et al* 2005 *Phys. Rev. Lett.* **95** 087203). It has been suggested that the magnetic properties of this material are described by a spin-1/2 Heisenberg model on the kagome lattice with spatially anisotropic exchange couplings. We report on investigations of the $\text{Sp}(\mathcal{N})$ symmetric generalization of this model in the large \mathcal{N} limit. We obtain a detailed description of the dependence of possible ground states on the anisotropy and on the spin length S . A fairly rich phase diagram with a ferrimagnetic phase, incommensurate phases with and without long-range order and a decoupled chain phase emerges.

1. Introduction

The magnetic lattice of the natural antiferromagnet volborthite consists of Cu^{2+} ions which occupy well separated planar kagome-like nets. A monoclinic distortion leads to a slight difference between the exchange couplings along one lattice direction (J) and the two other directions (J') within the planes. In this study, we consider the appropriate model, the Heisenberg antiferromagnet on the kagome lattice with spatial anisotropy (see figure 1),

$$\mathcal{H} = \sum_{\text{n.n.}} J_{ij} \mathbf{S}_i \cdot \mathbf{S}_j \quad \text{with } J_{ij} = \begin{cases} J & \text{if } i \text{ and } j \notin c\text{-sublattice} \\ J' = 1 & \text{otherwise.} \end{cases} \quad (1)$$

We have applied the spin wave approximation to this model, have done quantum perturbation theory around trial ground states, and have studied the $\text{Sp}(\mathcal{N})$ generalization in the limit of large \mathcal{N} where the mean-field approximation becomes exact [5]. Here, we report the results of the $\text{Sp}(\mathcal{N})$ -symmetric model. We consider this model in the full range of the anisotropy $0 \leq J \leq \infty$ and pay particular attention to possible transitions between different phases of the model which are expected to occur when J is varied.

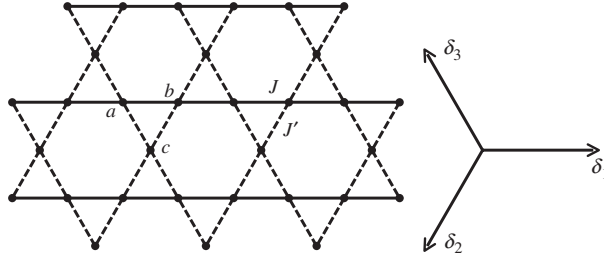


Figure 1. Anisotropic kagome model. The coupling J' will be set equal to unity. δ_ν , $\nu = 1, 2, 3$, are the primitive lattice vectors of the kagome net.

2. $\text{Sp}(\mathcal{N})$ approach

In this section, we sketch the mean field treatment of the $\text{Sp}(\mathcal{N})$ generalization of the model (1). The procedure follows closely that of [6, 7]. Further details can also be found in [5]. The first step is the replacement of the $SU(2)$ invariant product $\mathbf{S}_i \cdot \mathbf{S}_j$ in (1) by the $\text{Sp}(\mathcal{N})$ -symmetric expression $\frac{1}{\mathcal{N}} (\mathcal{J}_{\alpha\beta} b_i^\dagger{}^\alpha b_j^\dagger{}^\beta) (\mathcal{J}^{\gamma\delta} b_{i\gamma} b_{j\delta})$, where $b_{i\alpha}$, $b_i^\dagger{}^\alpha$ are bosonic operators and \mathcal{J} is the \mathcal{N} -dimensional generalization of the antisymmetric unit tensor in two dimensions [6, 7]. Here, we have introduced a paired index notation, $\alpha = (m, \sigma)$, $m = 1, \dots, \mathcal{N}$, $\sigma = \uparrow, \downarrow$ for the spinor index of the bosonic operators. The boson occupation numbers $n_b = b_i^\dagger{}^\alpha b_{i\alpha}$ are subject to the constraint

$$\kappa = n_b / \mathcal{N} \quad (2)$$

with κ a fixed parameter [7]. For the $SU(2)$ case, $\mathcal{N} = 1$, one has $\kappa = 2S$ with S the spin length. Hence, large values of κ , equivalent to large values of S in the $SU(2)$ model, correspond to the classical limit and small values of κ correspond to the quantum regime. The next step is a decoupling of the quartic terms in the Hamiltonian by a Hubbard–Stratonovich transformation using fields Q_{ij} which are defined on the links of the lattice. Additional fields λ have to be introduced as Lagrange multipliers to enforce the constraints (2) on the sites. We assume that the link variables are identical on all horizontal links of figure 1, $|Q_{ab}| = Q_1$, and on all diagonal links of figure 1, $|Q_{ac}| = |Q_{bc}| = Q_2$. Furthermore, we assume that $\lambda = \lambda_a$ on the a and b sites in figure 1, and $\lambda = \lambda_c$ on the c sites. Now, the bosons can be integrated out exactly. Then, in the large \mathcal{N} limit, the physical values of the variables Q_1 , Q_2 , λ_a , and λ_c are determined by the saddlepoint of the mean field energy

$$\frac{E_{\text{MF}}}{\mathcal{N}N_\nabla} = J |Q_1|^2 + 2 |Q_2|^2 - (2\lambda_a + \lambda_c)(\kappa + 1) + \frac{1}{N_\nabla} \sum_{\mathbf{k}, \mu} \omega_\mu(\mathbf{k}) (1 + |x_\mu(\mathbf{k})|^2) \quad (3)$$

with respect to these variables. Here, N_∇ is the number of downward pointing triangles of the lattice. The spinon frequencies $\omega_\mu(\mathbf{k})$, $\mu = 1, 2, 3$, are obtained as the three positive solutions of $\det \hat{\mathbf{D}}(\omega) = 0$, where $\hat{\mathbf{D}}(\omega)$ is the six-dimensional matrix related to the bosonic part of the $\text{Sp}(\mathcal{N})$ Hamiltonian after the Hubbard–Stratonovich transformation has been performed:

$$\hat{\mathbf{D}}(\omega) = \begin{pmatrix} \lambda_a - \omega & 0 & 0 & 0 & \tilde{Q}_2(\mathbf{k}) & J\tilde{Q}_1(\mathbf{k}) \\ 0 & \lambda_c - \omega & 0 & \tilde{Q}_2(\mathbf{k}) & 0 & \tilde{Q}_3(\mathbf{k}) \\ 0 & 0 & \lambda_a - \omega & J\tilde{Q}_1(\mathbf{k}) & \tilde{Q}_3(\mathbf{k}) & 0 \\ 0 & \tilde{Q}_2^*(\mathbf{k}) & J\tilde{Q}_1^*(\mathbf{k}) & \lambda_a + \omega & 0 & 0 \\ \tilde{Q}_2^*(\mathbf{k}) & 0 & \tilde{Q}_3^*(\mathbf{k}) & 0 & \lambda_c + \omega & 0 \\ J\tilde{Q}_1^*(\mathbf{k}) & \tilde{Q}_3^*(\mathbf{k}) & 0 & 0 & 0 & \lambda_a + \omega \end{pmatrix}, \quad (4)$$

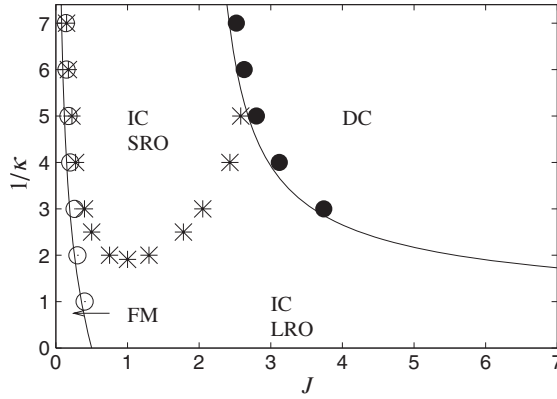


Figure 2. Phase diagram: FM, ferrimagnetic phase; IC, incommensurate phase; DC, decoupled-chain phase; empty circles, full circles and asterisks, numerical results; full lines, analytical results. Asterisks mark the boundary between phases with long-range order (LRO) and short-range order (SRO).

with $\tilde{Q}_\mu(\mathbf{k}) = iQ_\mu \sin(\delta_\mu \mathbf{k}/2)$, $\mu = 1, 2, 3$, and $Q_3 = Q_2$. In the above formula, the matrix elements $\tilde{Q}_\mu(\mathbf{k})$ incorporate information on the lattice symmetries via the primitive lattice vectors δ_μ of the kagome net (see figure 1) and the wavevector \mathbf{k} . The quantity $|x_\mu(\mathbf{k})|^2$ represents the density of Bose condensate that will develop at those points in the Brillouin zone where one of the spinon frequencies vanishes. By calculating the $\text{Sp}(\mathcal{N})$ analogue of the spin-spin correlation function, we can show that the long distance behaviour of this function is directly related to the existence of a condensate [5]: a finite condensate density, $|x_\mu(\mathbf{k})|^2 > 0$, implies long-range order (LRO), while for $|x_\mu(\mathbf{k})|^2 = 0$ there is only short-range order (SRO).

To find the saddle point of E_{MF} , (3), in the space of the variables $Q_1, Q_2, \lambda_a, \lambda_c$ and $|x_\mu(\mathbf{k})|^2$ at a given pair of parameters J, κ , we use an iterative numerical routine. Remarkably, and in contrast to previous applications of the mean field $\text{Sp}(\mathcal{N})$ approach [6–8], it turns out to be indispensable to allow for two independent Lagrange multipliers λ_a and λ_c . In view of the anisotropy of our model this is plausible.

3. Results and discussion

The results of the large- \mathcal{N} approach are summarized in the zero temperature phase diagram of the anisotropic kagome antiferromagnet. It displays the phases that we were able to discern in the $J-1/\kappa$ plane. We first note that, as expected, LRO which is always present for large κ disappears from the incommensurate (IC) phase for sufficiently small values of κ . Recall that for large κ we are in the classical regime of our model. The phase boundary that separates the region with SRO from the region with LRO was found by determining for each value of J that value of κ where the gap in the lowest branch of the one-spinon spectrum $\omega_\mu(\mathbf{k})$ first vanishes as κ is increased. At larger values of κ , condensate, and hence LRO, will appear. Since our model is maximally frustrated for $J = 1$, one expects a maximal suppression of LRO by quantum effects at this point. As is seen in figure 2, this is confirmed in the large- \mathcal{N} approach. For $J = 0$, the exact quantum ground state of our model (1) is ferrimagnetic (FM) according to the Lieb–Mattis theorem [9]. The classical ferrimagnet has all spins on the horizontal lattice lines aligned ferromagnetically while the middle spins are oriented antiparallel to these. In the classical limit, $\kappa \rightarrow \infty$, of our $\text{Sp}(\mathcal{N})$ model, the expectation value $Q_1 = \langle \mathcal{J}^{m\sigma m'\sigma'} b_{a m\sigma}^\dagger b_{b m'\sigma'} \rangle$, which

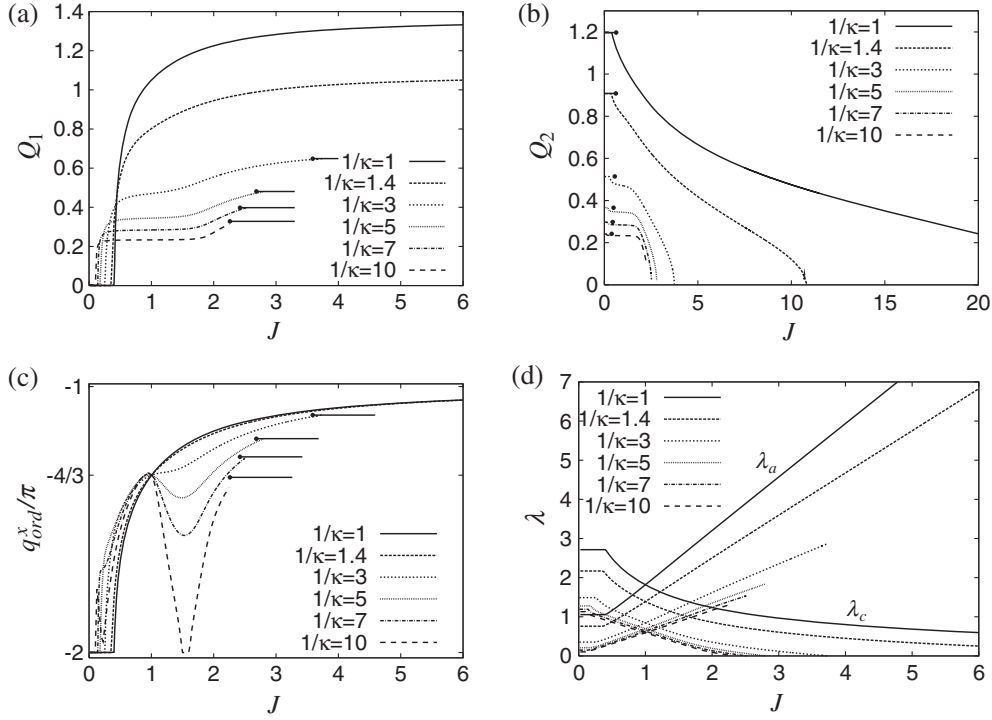


Figure 3. Saddlepoint values of the parameters Q_1 , Q_2 , of the ordering wavenumber q_{ord}^x ($q_{\text{ord}}^y = 0$), and of λ_a and λ_c . Full circles and horizontal lines in panels (a)–(c) are results of analytical determination of the saddlepoint.

measures the singlet weight on the horizontal bonds, should vanish in this state for sufficiently small J , $J \leq J_{\text{FM}}(\kappa)$. As J is increased beyond J_{FM} , Q_1 increases in the manner of an order parameter at a second order phase transition (see panel (a) of figure 3). At the same time, the parameter Q_2 begins to decrease, and it drops to zero at $J = J_{\text{DC}}(\kappa)$ (see panel (b) of figure 3). (Note that the J scales are different in panel (a) and panel (b).) Thus, the large- \mathcal{N} approach predicts the existence of a decoupled-chain phase in the region above the phase boundary J_{DC} . Q_2 decreases to zero continuously so that the phase transition at J_{DC} appears to be of second order again. Both LRO and SRO phases may be characterized by an ordering wavevector $\mathbf{q}_{\text{ord}} = 2\mathbf{k}_{\text{min}}$, where \mathbf{k}_{min} is that wavevector at which the lowest branch of the one-spinon excitation spectrum $\omega_\mu(\mathbf{k})$ has its minimum. The static spin structure factor $S(\mathbf{q})$ develops a peak at \mathbf{q}_{ord} . We display \mathbf{q}_{ord} in panel (c) of figure 3. For $J < J_{\text{FM}}(\kappa)$ we find $q_{\text{ord}}^x = -2\pi$ which is equivalent to $\mathbf{q}_{\text{ord}} = 0$. For $J > J_{\text{FM}}(\kappa)$, q_{ord}^x increases with J , and it reaches the value $-4\pi/3$ at the isotropic point $J = 1$. There it is independent of the value of κ in agreement with [7]. For $\kappa \gtrsim 1/3$, the behaviour of q_{ord}^x as a function of J is as expected: it increases monotonically towards $|q_{\text{ord}}^x| = \pi$ as $J \rightarrow \infty$. However, for $\kappa \lesssim 1/3$, the function $q_{\text{ord}}^x(J)$ develops a minimum at $J \approx 1.5$ which becomes more pronounced as κ decreases, i.e. as the importance of quantum effects increases. At present we have no physical explanation for this behaviour of \mathbf{q}_{ord} . The behaviour of the saddlepoint values of the Lagrange multipliers λ_a and λ_c as functions of J is displayed in panel (d) of figure 3 for various values of κ . As we have emphasized above, $\lambda_a \neq \lambda_c$ for general anisotropy, $J \neq 1$. Only at the isotropic point do we find $\lambda_a(\kappa) = \lambda_c(\kappa)$ in accordance with the expectation. Again, we have no intuitive physical

explanation for the behaviour of these parameters as functions of J and κ . Quite unexpectedly λ_c drops to zero at the boundary J_{DC} of the DC phase.

In the vicinity of the FM–IC and the IC–DC phase boundary, where Q_1 , respectively Q_2 , are small one can expand E_{MF} , (3), with respect to these variables and solve the extremum problem analytically. The expansion reads

$$E_{\text{MF}}(Q_\alpha) = e_{0\alpha} + r_\alpha |Q_\alpha|^2 + g_\alpha |Q_\alpha|^4 + \mathcal{O}(|Q_\alpha|^6), \quad (5)$$

where $\alpha = 1(2)$ for the FM–IC(IC–DC) phase boundary. After the stationarity conditions $E_{\text{MF}}(Q_\alpha)$ with respect to the variables Q_β , $\beta = 2(1)$, λ_a , λ_c have been solved the coefficients $r_{0\alpha}$ and g_α are known as functions of J and κ . Our numerical results suggest that $g_\alpha > 0$. Similar to a Landau–Ginzburg expansion, the FM–IC and the IC–DC phase boundaries are then obtained as the solutions of $r_{\alpha 0} = 0$. These solutions are presented as solid lines in figure 2. Obviously, the numerical data agree reasonably well with these analytical solutions. Small discrepancies arise in the numerical data because the energy surface $E_{\text{MF}}(Q_1, Q_2, \lambda_a, \lambda_c)$ is very shallow in the vicinity of the saddle point. On these boundaries and inside the FM and the DC phases the values of Q_1 , Q_2 and of the ordering wavevector remain constant as is shown in the corresponding panels of figure 3. Using a similar expansion technique for the $\text{Sp}(\mathcal{N})$ analogue of the spin–spin correlation function, we have also been able to obtain the asymptotic behaviour of this function on the phase boundaries analytically. We find that there is indeed LRO along the entire phase boundaries up to arbitrarily small values of κ . However, while along the FM–IC phase boundary there is LRO between any pair of spins $\mathbf{S}_{\mu i}$, $\mathbf{S}_{\nu j}$, $\mu, \nu = a, b, c$, along the IC–DC phase boundary there is LRO only between the spins on the c sites \mathbf{S}_{ci} , see figure 1.

To conclude, we wish to compare the results presented here for the anisotropic kagome antiferromagnet (AF), (1), with those obtained by Chung *et al* [8] for the $\text{Sp}(\mathcal{N})$ -symmetric generalization of the anisotropic triangular AF. With increasing values of J , which controls the anisotropy in both models, we find the same succession of phases as in [8]: a collinear phase, an incommensurate phase and a decoupled chain phase. However, while LRO disappears for sufficiently small values of $\kappa = 2S$ for all values of J in the triangular AF, we find LRO in the entire FM phase and along the FM–IC and the IC–DC phase boundaries up to arbitrarily small values of κ . For both models, the mean-field $\text{Sp}(\mathcal{N})$ approach predicts a DC phase which, however, is certainly not described faithfully by this approach. Qualitative consideration of the role of fluctuations in this phase led the authors of [8] to the conclusion that there is spin Peierls order in the DC regime of the anisotropic triangular AF. Such a picture is still elusive for the anisotropic kagome AF. However, by applying perturbation theory to the trimerized version of the model (1), i.e. to a model for which the couplings on, for example, the upward pointing triangles are uniformly weaker than those on the downward pointing triangles [10], we find that for $J \gg 1$ the dynamics of the c spins of our model (see figure 1) is effectively described by the Hamiltonian of the anisotropic triangular AF with strong coupling in one of the three lattice directions. Therefore, according to the arguments of [8], there should be spin Peierls order between these spins. Since, on account of the trimerization, the spins on the a and b sites in figure 1 are already paired in nearest neighbour singlet pairs, one may thus speculate that spin Peierls order also prevails in the DC phase of the anisotropic kagome AF.

Acknowledgments

One of the authors (HUE) acknowledges a useful discussion with F Mila. The work at the University of Waterloo was supported by the Canada Research Chair (Tier I, Michel Gingras).

References

- [1] Hiroi Z *et al* 2001 *J. Phys. Soc. Japan* **70** 3377
- [2] Fukaya A *et al* 2003 *Phys. Rev. Lett.* **91** 207603
- [3] Bert F *et al* 2004 *J. Phys.: Condens. Matter* **16** S829
- [4] Bert F *et al* 2005 *Phys. Rev. Lett.* **95** 087203
- [5] Yavors'kii T, Apel W and Everts H U 2006 in preparation
- [6] Sachdev S and Read N 1991 *Int. J. Mod. Phys. B* **5** 219
- [7] Sachdev S 1992 *Phys. Rev. B* **45** 12377
- [8] Chung C H, Marston J B and McKenzie R H 2001 *J. Phys.: Condens. Matter* **13** 5159
- [9] Lieb E H and Mattis D C 1992 *J. Math. Phys.* **3** 749
- [10] Mila F 1998 *Phys. Rev. Lett.* **81** 2356